Available online at www.sciencedirect.com

ScienceDirect

www.elsevier.com/locate/jmbbm

Research Paper

Quantification of nonlinear elasticity for the evaluation of submillimeter crack length in cortical bone

Sylvain Haupert[a,*], Sandra Guérard[b], David Mitton[c,d,e], Françoise Peyrin[f,g,h,i], Pascal Laugier[a]

[a]Sorbonne Universités, Université Pierre et Marie Curie, CNRS UMR7371 & INSERM U1146, Laboratoire d'Imagerie Biomédicale, Paris FR-75006, France
[b]Arts et Métiers ParisTech, LBM, 151 Boulevard de l'Hôpital, Paris, France
[c]Université de Lyon, F-69622 Lyon, France
[d]Université Claude Bernard Lyon 1, Villeurbanne, France
[e]IFSTTAR, UMR_T9406, LBMC Laboratoire de Biomécanique et Mécanique des Chocs, F69675 Bron, France
[f]CREATIS, CNRS UMR 5220, Inserm, U1044, Université de Lyon; Université Lyon 1, INSA-Lyon; 69621, Villeurbanne, France
[g]European Synchrotron Radiation Facility, X-Ray Imaging Group, 38043 Grenoble, France
[h]Université Lyon I, Lyon, France
[i]ESRF, Grenoble, France

ARTICLE INFO

Article history:
Received 20 November 2014
Received in revised form
8 April 2015
Accepted 12 April 2015
Available online 22 April 2015

Keywords:
Cortical bone
Crack
Damage
Elasticity
Nonlinear acoustics
Nonlinear resonant ultrasound spectroscopy

ABSTRACT

The objective of this study was to investigate the sensitivity of the nonlinear elastic properties of cortical bone to the presence of a single submillimetric crack. Nonlinear elasticity was measured by nonlinear resonant ultrasound spectroscopy (NRUS) in 14 human cortical bone specimens. The specimens were parallelepiped beams ($50 \times 2 \times 2$ mm^3). A central notch of 500 μm was made to control crack initiation and propagation during four-point bending. The nonlinear hysteretic elastic and dissipative parameters α_f and α_Q, and Young's modulus E_{us} were measured in dry condition for undamaged (control) specimens and in dry and wet conditions for damaged specimens. The length of the crack was assessed using synchrotron radiation micro-computed tomography (SR-μCT) with a voxel size of 1.4 μm. The initial values of α_f, measured on the intact specimens, were remarkably similar for all the specimens ($\alpha_f = -5.5 \pm 1.5$). After crack propagation, the nonlinear elastic coefficient α_f increased significantly ($p < 0.006$), with values ranging from −4.0 to −296.7. Conversely, no significant variation was observed for α_Q and E_{us}. A more pronounced nonlinear elastic behavior was observed in hydrated specimens compared to dry specimens ($p < 0.001$) after propagation of a single submillimetric crack. The nonlinear

*Corresponding author.
E-mail address: sylvain.haupert@upmc.fr (S. Haupert).

http://dx.doi.org/10.1016/j.jmbbm.2015.04.013

Synchrotron radiation micro-computed tomography

elastic parameter α_f was found to be significantly correlated to the crack length both in dry ($R=0.79$, $p<0.01$) and wet ($R=0.84$, $p<0.005$) conditions. Altogether these results show that nonlinear elasticity assessed by NRUS is sensitive to a single submillimetric crack induced mechanically and suggest that the humidity must be strictly controlled during measurements.

1. Introduction

This study focuses on bone microdamage and particularly on the microcracks that are thought to play an important role in bone strength (Burr et al., 1998; Diab and Vashishth, 2005; Hernandez et al., 2014; Yeni and Fyhrie, 2002), toughening mechanisms (Diab and Vashishth, 2005; Fletcher et al., 2014; Vashishth, 2004; Yeni and Fyhrie, 2002) and remodeling (Cardoso et al., 2009; Verborgt et al., 2000). The link between microcracks and bone fracture is not fully elucidated yet (Burr, 2011; Chapurlat and Delmas, 2009; Gupta and Zioupos, 2008), though microdamage is suspected to be at the origin of some spontaneous fractures (Shane et al., 2010).

The quantitative assessment of damage characteristics remains challenging. Histomorphometry is the gold standard, although providing only 2-D damage characterization (Lee et al., 2003; O'Brien et al., 2007, 2002). New techniques are emerging, such as synchrotron radiation micro-computed tomography (SR-μCT) (Haupert et al., 2014; Larrue et al., 2011; Voide et al., 2009). However, none of these invasive techniques can be applied in vivo, nor is able to assess damage in a large bone volume. Consequently there is a clear need for alternative techniques to assess bone microdamage.

Nonlinear acoustics methods have been introduced recently for the investigation of bone microdamage. They include nonlinear resonant ultrasound spectroscopy (NRUS) (Haupert et al., 2014; Muller et al., 2008), nonlinear wave modulation spectroscopy (NWMS) (Ulrich et al., 2007) and dynamic acousto-elastic testing (DAET) (Moreschi et al., 2011; Renaud et al., 2008). These approaches, directly inspired from nonlinear elastic wave spectroscopy (NEWS) methods developed in the field of nondestructive testing of materials, have been reported to be sensitive to fatigue-induced damage in materials such as concrete (Antonaci et al., 2010; Chen et al., 2010; Van den Abeele and De Visscher, 2000), metals (Cantrell, 2006; Cantrell and Yost, 2001; Frouin et al., 1999; Kim et al., 2006, 2004; Nagy, 1998; Sagar et al., 2011; Zagrai et al., 2008) or composites (Aymerich and Staszewski, 2010; Bentahar and El Guerjouma, 2009; Meo et al., 2008; Van den Abeele et al., 2009, 2001b). However, so far, few studies have attempted to quantify microdamage, using nonlinear acoustic methods (Moreschi et al., 2011; Van den Abeele et al., 2009, 2001a). Haupert et al. (2014) have investigated the relationship between the nonlinear elastic behavior measured by NRUS and fatigue-induced microdamage of cortical bone specimens, taking advantage of micrometer resolution imaging by SR-μCT. With this approach, the study evidenced a significant correlation between the variation of bone microcrack density and the variation of nonlinear elasticity. These findings not only revealed the sensitivity of NRUS to early bone microdamage, but also established the first quantitative relationship between the variation of nonlinear elasticity of bone and variation of a microcrack characteristic.

A complementary vision to the fatigue test is to produce damage locally by initiating and propagating a single crack in a controlled manner. In this study, calibrated specimens of human cortical bone undergoing a toughness test were measured by NRUS and then imaged by SR-μCT. Our main objective was to investigate whether the nonlinear elastic behavior or the elastic modulus are changed after propagation of a localized single crack and to specifically assess the relationship between the nonlinear elastic behavior and the length and the orientation of the crack. This was achieved by comparing NRUS measurements on native and cracked specimens in dry condition. An ancillary objective was to investigate the influence of hydration on the nonlinear response. To this goal, NRUS testing was performed on cracked specimens in dry and wet conditions.

2. Methods

2.1. Specimen preparation

Fourteen human cortical bone specimens were prepared from the femoral mid-diaphysis of four donors (age = 79.4 ± 3.9). Ethical approval for the collection of samples was granted by the Human Ethics Committee of the Département Universitaire d'Anatomie de Rockfeller (Lyon, France). The tissue donors or their legal guardians provided informed written consent to give their tissue for investigation, in accord with legal clauses stated in the French Code of Public Health. Parallelepiped beams-shaped specimens ($50 \times 2 \times 2\ mm^3$) were wet machined (Isomet 4000, Buehler GmbH, Düsseldorf, Germany) oriented along the proximal to distal direction of the femur. Then they were notched by a diamond wire saw (ESCIL W3000, Chassieu, France) in their middle to form a notch of roughly a quarter of the specimen width (i.e. 500 μm). The notch orientation was such that the nominal crack-growth direction for subsequent toughness testing was transverse to the long axis of the specimen, in a direction perpendicular to the osteon alignment. All specimens were defatted for 12 h in a chemical bath of

diethylether and methanol (1:1) and stored at −20 °C until experiments.

Apparent dry density (ρ_{dry}) was evaluated by measuring the specimen volume and weight. Bone specimens were dried at 37 °C during 12 h in a climate chamber (Memmert GmbH HCP 108, Schwabach, Germany) at relative humidity below 20% in the presence of desiccators. According to several authors, collagen molecular structure remains intact during drying and rewetting procedures, so that this protocol is believed not to affect bone properties (Currey, 1988; Rho and Pharr, 1999).

2.2. Measurement protocol

The experimental protocol began with the NRUS measurements to determine the initial elastic nonlinearity of the dry notched specimens. Previous NRUS measurements on cortical bone (Haupert et al., 2014, 2011; Muller et al., 2008) were all performed on dry specimens. In the present study, we kept measuring bone specimens in dry condition in order to compare the results with previous reports. The specimens were then taken through a toughness test in wet conditions. Crack initiation and growing was carefully controlled to avoid the rupture of the specimens. NRUS measurements were repeated after the toughness test for all the cracked specimens in dry condition (i.e. relative humidity < 20%). Because some studies have evidenced that the nonlinear elastic response of materials such as concrete and rocks is influenced by the level of hydration (Johnson et al., 2004; Payan et al., 2010; Van den Abeele et al., 2002), NRUS measurements were repeated on the cracked specimens in wet condition (i.e. relative humidity > 80%). Finally, the crack length was estimated using SR-μCT. The sequence of measurement steps is illustrated on Fig. 1.

2.3. NRUS measurements

When damaged materials are subjected to a dynamic loading, the elastic modulus decreases as strain amplitude increases. A typical manifestation of this phenomenon, the so-called "softening effect", is the decreasing of the resonance frequency of the first compression modes (Haupert et al., 2011) when the excitation amplitude increases. In addition, the Q-factor of the resonance peak, defined as the ratio of the resonance frequency to the resonant peak width at half-maximum, also decreases for increasing excitation amplitudes. This behavior, which is typical of the non-linear non-classical elastic behavior (Guyer and Johnson, 2009), also known as hysteretic elasticity, of damaged materials appears for strains above approximately 10^{-5} (Johnson and Sutin, 2005). It conveys information about the amount of hysteretic nonlinear units representing the damaged zones in the material.

The principles of NRUS measurements have been extensively described elsewhere (Van den Abeele et al., 2000). The protocol was adapted to achieve high sensitivity to detect small variations of bone nonlinear parameters (Haupert et al., 2011). Briefly, a piezoceramic emitter (Fuji Ceramics Corporation, Yamamiya, Japan) glued on a backload was bonded at one end of the specimen to ensure it is in free–fix boundary condition for NRUS measurements. Such boundary conditions impose a null displacement (i.e. maximum strain) at the fixed end of the specimen and a maximum displacement (i.e. null strain) at its free end. Each specimen was probed by a swept-sine (M2i.6612, Spectrum GmbH, Grosshansdorf, Germany) encompassing the first resonant mode of the cortical beam (assumed to be pure compression mode under asymmetric boundary conditions). The peak resonance frequency f and energy loss Q^{-1} were measured as a function of strain applying increasing voltage drive level. Two hysteretic nonlinear elastic (α_f) and dissipative (α_Q) parameters, related to the frequency shift Δf and to the energy loss variation (ΔQ^{-1}) as a function of strain, respectively, were extracted as follows (Van den Abeele et al., 2000):

$$\frac{f-f_0}{f_0}=\frac{\Delta f}{f_0}=\frac{\alpha_f}{2}\Delta\varepsilon \tag{1}$$

$$\frac{1}{Q}-\frac{1}{Q_0}=\frac{\alpha_Q}{2}\Delta\varepsilon \tag{2}$$

where f and Q are the resonance frequency and Q-factor at increased strain level, f_0 and Q_0 are the reference values (assumed to be linear) at the lowest drive amplitude, $\Delta\varepsilon$ is the maximal dynamic strain level over a period. The dynamic strain amplitude ε was calculated from the longitudinal particle displacement U at the free end of the specimen measured by a laser vibrometer (LSV 1 MHz, SIOS, Ilmenau, Germany):

$$\varepsilon=\frac{\delta U}{\delta x}=Uk=U\frac{2\pi}{4L} \tag{3}$$

where k is the wave number and L is the specimen length.

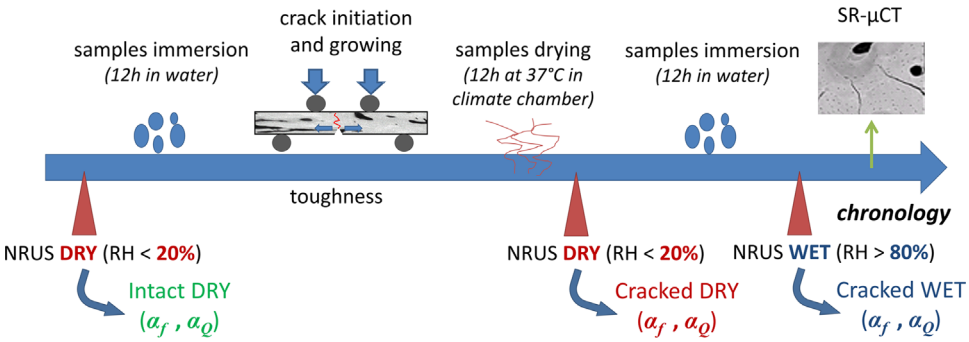

Fig. 1 – Diagram illustrating the measurement protocol.

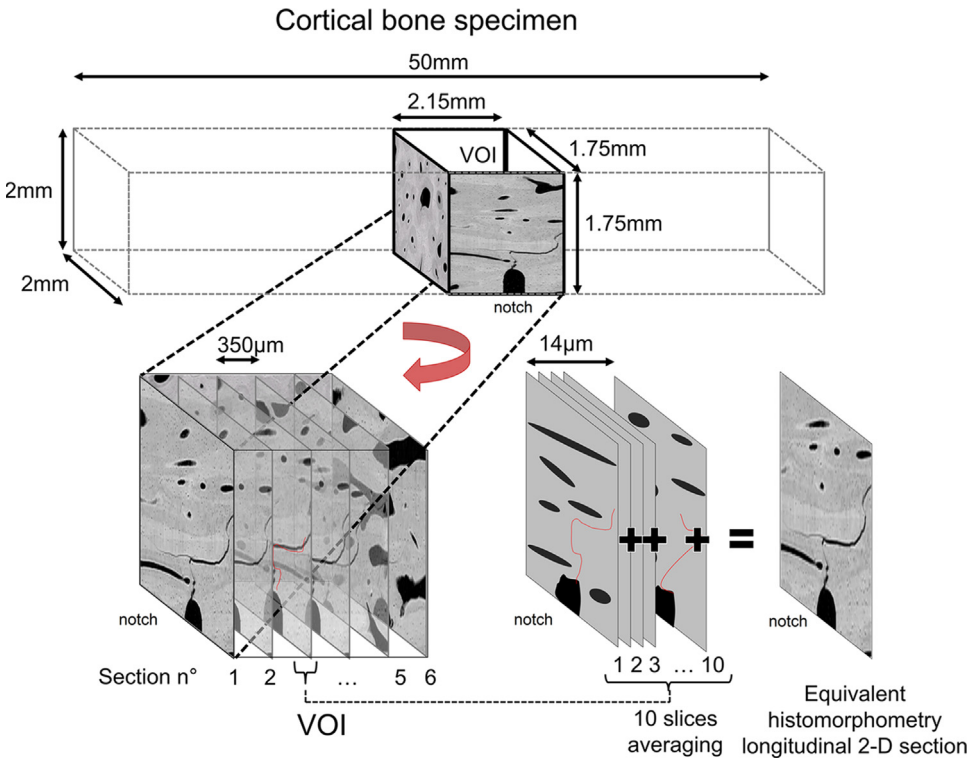

Fig. 2 – Diagram illustrating the process leading to an equivalent histomorphometric 2-D transverse cross-section image from 3-D reconstructed bone volumes acquired by SR-µCT.

Both nonlinear elastic α_f and dissipative α_Q parameters were evaluated on intact and cracked specimens in dry condition. During NRUS measurements, specimens were kept at fixed temperature (37 ± 0.1 °C).

Given the free–fix boundary conditions for NRUS measurements, the resonance mode is such that the length of the specimen L equals a quarter of the wavelength at the corresponding resonance frequency ($\lambda = 4L$). Thus, the sound velocity c_0 can be estimated by:

$$c_0 = 4Lf_0 \quad (4)$$

As the wavelength λ is much larger than the characteristic dimension of the cross section of the specimens, the wave propagates in the specimens according to the bar mode. Thus, the ultrasonic Young's modulus (E_{us}) can be estimated by (Achenbach, 1984; Grimal et al., 2009):

$$E_{us} = \rho_{dry} {c_0}^2 \quad (5)$$

2.4. Toughness testing

The piezoceramic emitter attached to the specimen was removed before mechanical testing. To be closer to realistic in-vivo cracking conditions, the notched specimens were hydrated into saline during 12 h. The wet specimens were monotonically loaded at a displacement rate of 0.05 mm/s with a preload of −4 N, using a crack opening (mode I) four-point bending setup. The test was stopped before failure at different crack lengths. The test was conducted on wet specimens in the air, at ambient temperature, using a hydraulic testing machine (INSTRON, 8802, High Wycombe, England) with a 1 kN loading cell (accuracy 0.5%) and the internal displacement transducer (accuracy 1%). The specific four-point bending assembly is composed of 6.35 mm diameter roller-bearings with a 40 mm outer span and a pivoting 20 mm inner span. In this configuration, the formation of grooves under the rollers is minimized (Griffin et al., 1997).

2.5. 3-D synchrotron radiation µCT (SR-µCT)

After NRUS measurements and mechanical testing, the samples were measured by SR-µCT at the European Synchrotron Radiation Facility (Grenoble, France) on beam-line ID19 following the data acquisition protocol extensively presented in previous studies (Haupert et al., 2014; Larrue et al., 2011). The photon energy was 25 keV and the size of the measured volume was $2.8 \times 2.8 \times 1.96$ mm^3 with a voxel size of 1.4 µm^3.

For crack characterization, a sub volume of interest (VOI) of $2.15 \times 1.75 \times 1.75$ mm^3, encompassing the notch and the crack over the entire width of the sample, was analyzed. The VOI was sampled by 2-D longitudinal cross-sections regularly spaced with an interval of 350 µm (Fig. 2). Each cross-section was obtained by averaging a stack of 10 adjacent 1.4 µm-thick slices in order to decrease the noise level and improve the contrast between the crack and the bone matrix (Fig. 2).

For crack length determination, only the main crack starting at the notch was considered, while all peripheral microcracks that were not connected to the main crack were removed to avoid including bias in the analysis. Crack length was manually determined by approximating the main crack as a succession of line segments. The total crack length was

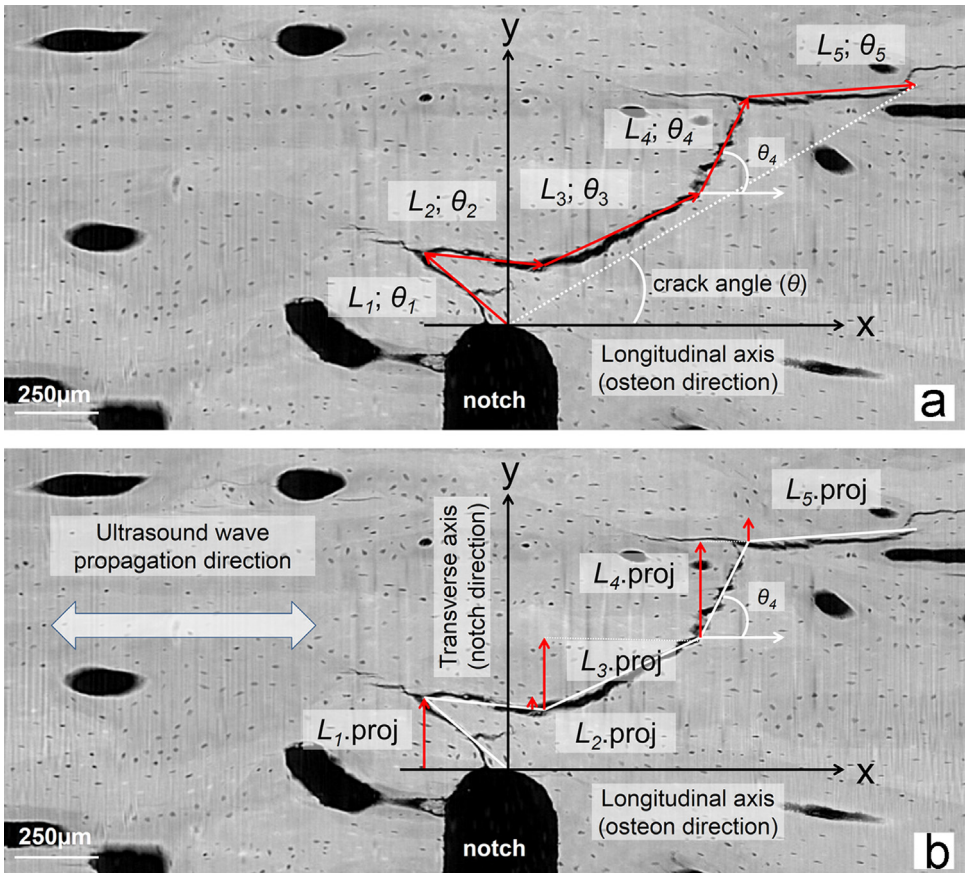

Fig. 3 – (a) Decomposition of the main crack into 5 vectors with lengths L_n and angles θ_n. The crack length Cr.Le=L_1+L_2+L_3+L_4+L_5. The mean crack angle is estimated in a coordinate system composed by the osteon direction (*x* axis) and the notch direction (*y* axis). It corresponds to the vector orientation between both extremities of the main crack. (b) The orthogonal projection of the main crack on the transverse axis corresponds to the sum of the 5 vectors projected on the same axis. Cr.Le.Proj=L_1.Proj+L_2.Proj+L_3.Proj+L_4.Proj+L_5.Proj (with L_n.Proj=L_n*sin (θ_n)).

Table 1 – Apparent density (ρ_{dry}), porosity, Young's modulus E_{US}, total mean crack length Cr.Le, mean angle, projected mean crack length Cr.Le.Proj, nonlinear elastic α_f and dissipative α_Q parameters before and after the toughness test and in dry and wet conditions.

Specimen	ρ_{dry} [g/cm^3]	Porosity [%]	Initial E_{US} [GPa]	Final E_{US} [GPa]	Cr. Le [µm]	Angle [°]	Cr. Le. Proj [µm]	Initial dry α_f	Final dry α_f	Final wet α_f	Initial dry α_Q	Final dry α_Q	Final wet α_Q
#1	1909	6.2	22.6	21.4	2277	17	664	−4.9	−296.7	−217.6	1.8	–	–
#2	1987		22.8		Failure			−4.4	Failure		1.6	Failure	
#3	1778	11.0	18.8	19.8	65	14	16	−5.5	−4.0	−6.2	2.1	2.0	1.5
#4	1867	7.8	21.6	22.2	208	33	112	−6.3	−10.8	−19.7	2.2	2.7	3.7
#5	1856		21.0		Failure			−5.0	Failure		1.4	Failure	
#6	1886	7.1	22.3	22.2	341	38	209	−4.1	−21.3	−21.5	1.5	2.7	4.0
#7	1847	8.5	21.0	20.6	738	26	318	−4.4	−20.2	−37.0	1.7	3.5	6.7
#8	1759	11.7	20.6	19.7	917	20	315	−5.8	−120.5	−119.1	0.7	–	–
#9	1744	12.2	19.9	19.8	104	21	37	−4.5	−6.3	−14.6	1.6	1.9	4.3
#10	1635	16.2	17.4	17.5	192	42	128	−7.1	−11.5	−17.5	1.5	2.4	2.0
#11	1762	11.6	20.8	21.0	6	81	6	−5.0	−5.6	−7.4	2.6	1.1	2.8
#12	1744	12.2	20.4	20.4	475	25	203	−4.4	−11.8	−28.7	1.6	1.8	4.5
#13	1877	7.4	21.5	21.3	547	13	126	−5.3	−16.0	−23.0	2.2	2.6	4.3
#14	1871	7.6	21.9	21.5	618	14	147	−10.0	−14.5	−17.8	3.1	2.6	4.3

estimated by summing the length of the line segments. A line segment *n* was represented by a vector of length L_n and angle θ_n. The total mean crack length (Cr.Le [µm]) was the average of the total crack lengths measured on six different longitudinal sections regularly sampling the VOI. The mean crack angle θ is estimated in a coordinate system composed by the osteon direction (x-axis) and the notch direction (y-axis). It corresponds to the vector orientation delimited by both extremities of the main crack. Lengths (L_n) and angles (θ_n) were measured using the software

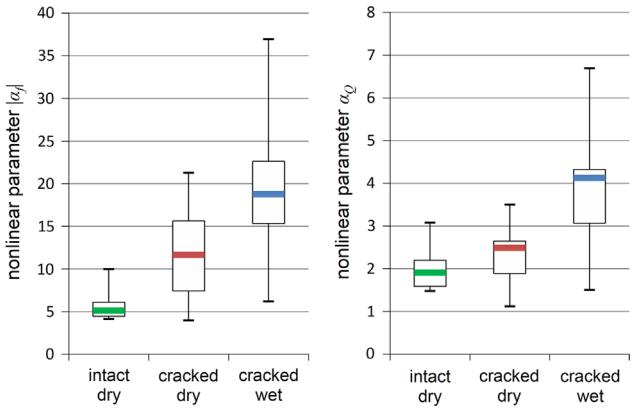

Fig. 4 – Nonlinear elastic α_f (a) and dissipative α_Q (b) before and after crack propagation, measured in dry and wet conditions. For the sake of clarity, the two outliers (#1 and #8) are not represented.

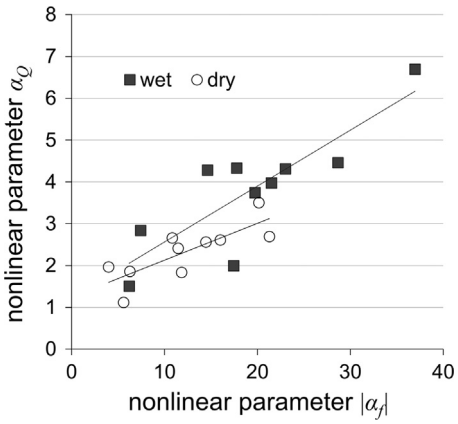

Fig. 5 – Correlation between the nonlinear elastic coefficient α_f and the nonlinear dissipative coefficient α_Q measured in dry and wet cortical bone specimens.

ImageJ (NIH, USA) with the plugin NeuronJ (Meijering, 2010). The length of the cracks projected in the notch direction, i.e. perpendicular to the ultrasound wave propagation, is Cr.Le.Proj (Fig.3). Cr.Le.Proj is the sum of the length projected on y-axis of all the line segments of the crack at 90° (L_n.Proj$=L_n$*sin(θ_n)) (Fig. 3).

The bone surface was computed as the total area of bone section, including the pores (Harversian and Volkmann canals, and resorption cavities) (Lee et al., 2000; Zioupos, 2001). The apparent bone porosity corresponds to pores appearing as dark pixels on SR-μCT cross-section images. The pores, visible as dark regions, were segmented using a low threshold value chosen heuristically, followed by an opening on the binary image to remove isolated pixels. Cortical porosity was derived as the ratio of the summed area of all pores to the total bone area, including pores.

2.6. *Data analysis*

Matlab 7.8 with statistics toolbox 7.6 (Mathworks, Natick, MA, USA) was used for statistical analyses. The difference between measurements (α_f and α_Q) before and after the mechanical testing, hydrated or dry, were assessed with a non-parametric Wilcoxon signed rank test on nonlinear parameters (α_f and α_Q). The relationship between nonlinear parameters (α_f and α_Q) and crack length (total Cr.Le and projected Cr.Le.Proj) was assessed using the Pearson correlation coefficient after checking for the normality of the parameters distributions. (Shapiro–Wilk test). The significance level was measured using a p-value $p<0.05$.

3. Results

3.1. *Evaluation of the crack length*

The characteristics measured for all the specimens are displayed in Table 1. The total length of the cracks varies from 6 μm to 2277 μm while the mean angle of the cracks (θ) varies from $\theta=13°$ to 81° (0° means an alignment with osteon direction) with a mean value of $27\pm19°$. The projected length (Cr.Le.Proj) of the cracks varies from 6 μmto 664 μm. Note that two specimens (#2 and #5) were fractured during the toughness test therefore data analysis was performed with 12 specimens.

3.2. *NRUS*

We remind that the measurement precision of NRUS was found to be 16.2% for α_f and 14.2% for α_Q in previously reported results (Haupert et al., 2011). The initial values of α_f and α_Q were remarkably similar for all the specimens and vary within a relatively narrow range: $\alpha_f=-5.5\pm1.5$ (min: −4.4; max: −10.0) and $\alpha_Q=1.8\pm0.6$ (min: 0.7; max: 3.1). After crack propagation, the nonlinear elastic coefficient α_f has increased significantly ($p<0.006$), with α_f values ranging from −4.0 to –296.7 (Fig. 4a). Two specimens manifested a huge increase of α_f (#1: α_f varies from −4.9 to −296.7; #8: α_f varies from −5.8 to −120.5). Two specimens (#3, #11) showed an insignificant change of α_f, compared to the technique precision,

In contrast, the values of α_Q after crack propagation, ranging between 1.1 and 3.5, remained close to the initial values and the variation did not reach a significant level. (Fig. 4b). The dissipative nonlinear α_Q could not be extracted for two specimens (#1 and #8). Indeed, in these two cases, there was no linear dependence between the strain level ε and the energy loss variation ΔQ^{-1} as expected from Eq. (2). For high strain level above $\varepsilon=10^{-4}$, the variation ΔQ^{-1} saturated. For these reasons, these two specimens were removed from the statistical analysis.

Finally, a statistically significant difference was found between both nonlinear coefficients (α_f $p=0.002$; α_Q $p=0.01$) between measurements achieved on cracked specimens under hydrated or dehydrated conditions, suggesting that hydration has an effect on nonlinear elasticity. Nonlinearity was higher under hydrated condition.

Both nonlinear hysteretic parameters measured after crack propagation, in dry and wet conditions, were significantly correlated (hydrated specimens: $R=0.78$ $p=0.007$; dehydrated specimens $R=0.85$, $p=0.002$) (Fig. 5).

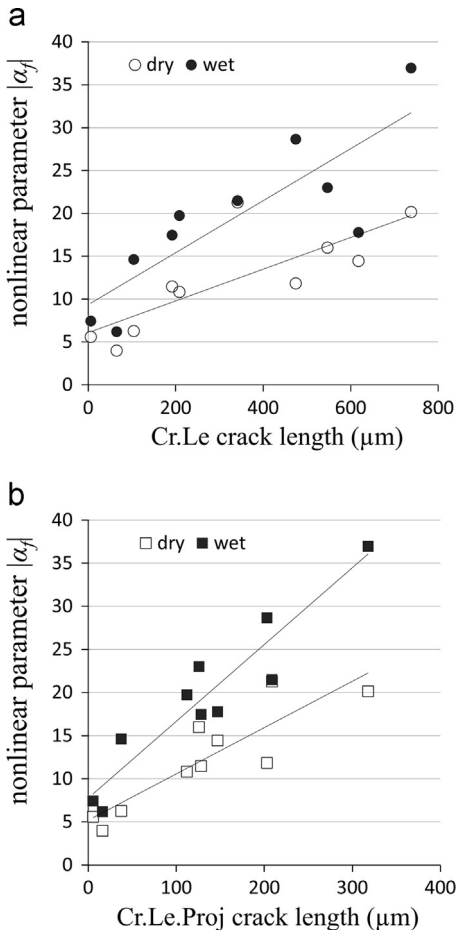

Fig. 6 – Correlation between the crack length (total Cr.Le (a) or projected Cr.Le.Proj (b)) and the nonlinear elastic coefficient α_f measured in dry and wet cortical bone specimens.

The nonlinear elastic parameter α_f was significantly correlated to Cr.Le (dehydrated $R=0.79$ $p<0.01$: hydrated $R=0.84$ $p<0.005$) and to Cr.Le.Proj (dehydrated $R=0.88$ $p<10^{-3}$; hydrated $R=0.94$ $p<10^{-4}$) (Fig. 6). Similarly, the nonlinear dissipative parameter α_Q was significantly correlated to Cr.Le (dehydrated $R=0.71$ $p=0.02$: hydrated $R=0.79$ $p<0.005$) and to Cr.Le.Proj (dehydrated $R=0.76$ $p=0.01$; hydrated $R=0.76$ $p=0.01$). There was no significant difference between the values of Young's modulus (E_{us}) measured before or after crack propagation

4. Discussion

To our best knowledge, this study represents the first investigation of the variations of linear (E_{us}) and nonlinear hysteretic elastic parameters (α_f, α_Q) of human cortical bone specimens after a crack initiation and propagation experiment. Similar studies have been reported, but in metal or in concrete (Courtney et al., 2008; Donskoy et al., 2001; Duffour et al., 2006; Straka et al., 2008; Zardan et al., 2010). Linear and nonlinear measurements of elastic properties were achieved on each specimen before and after crack propagation, so that each specimen was its own control. The results evidence an increase of the nonlinear hysteretic elastic coefficient α_f of the bone specimens after crack propagation in agreement with the results reported on different materials (Courtney et al., 2008; Duffour et al., 2006). Furthermore, we found a significant correlation between crack length and the nonlinear parameters α_f and α_Q, which is consistent with the recent results reported by Zardan et al. (2010) in concrete and Donskoy et al. (2001) in steel.

In contrast, the crack propagation has no measureable effect on the elastic modulus E_{us}. This suggests that the nonlinear hysteretic elastic behavior is more sensitive to the presence of a single crack than linear elasticity corroborating the result found in concrete by Zardan et al. (2010).

The values of α_f and α_Q measured in the specimens before crack initiation and propagation are in agreement with those observed in previous experiments conducted on human or bovine dry cortical bone (Haupert et al., 2014, 2011). However, the damaged specimens of the present study, with a single crack, exhibit values of α_f that are far higher than those measured in damaged specimens with an accumulation of non-localized microcracks occurring after a fatigue test (Haupert et al., 2014). During the fatigue test conducted in our previous study, the damage remained at an early stage of development resulting in the accumulation of tiny microcracks with a lower nonlinear responses compared to the current specimens. We hypothesize that the total volume of the accumulated microcracks, within which the nonlinear mechanisms may occur, is probably much less extended than the volume of a region damaged with a large crack. Future studies are required to gain insight into the role played by the volume occupied by cracks on the nonlinear elastic behavior.

We assume that the activation of the nonlinear elastic behavior by crack opening/closing processes is larger when the crack is perpendicular to the direction of propagation of the compression wave. As a consequence, the correlation of the nonlinear elastic behavior is expected to be stronger with the length of crack portions perpendicular to the wave direction than with the total crack length. Although our data showed a trend to a higher correlation of α_f with Cr.Le.Proj than with Cr.Le, the difference did not reach a statistically significant level ($Z<1.65$, Steiger's Z-test for correlated correlations (Meng et al., 1992)), probably because of the weak statistical power of the test due to the limited number of specimens included in the study. A larger sample size is needed to confirm this assumption.

The nonlinear elastic behavior was investigated under different hydration conditions upon the same set of cracked specimens. Both nonlinear hysteretic parameters increase after bone hydration (Fig. 4). The influence of hydration was also studied in rocks (Johnson et al., 2004; Tutuncu et al., 1998; Van den Abeele et al., 2002; Zinszner et al., 1997), woods (Derome et al., 2011) and concrete (Payan et al., 2010). In rocks, the nonlinear elastic behavior increases as the water content increases (Johnson et al., 2004) contrary to concrete (Payan et al., 2010). These observations are interpreted based on different mechanisms, such as 1) capillarity forces due to water (non-viscous) (Van den Abeele et al., 2002), 2) adhesion forces due to a viscous liquid between grain boundaries or cracks lips (Nazarov, 2001), or 3) fluid flow that modify the diameter of tubes where the fluid moves (Nazarov and Radostin, 2008). Whether such mechanisms may exist in cortical bone which can be considered as a matrix pervaded by a porous network filled with viscous fluids, in the

specific case of bone, collagen with hydration-dependent elastic properties (Rho and Pharr, 1999) may be another factor that has to considered. From an experimental point of view, this result has important consequence as it suggests that humidity must be strictly controlled during measurement.

The nonlinear dissipative parameter α_Q was measured concurrently with the nonlinear elastic parameter α_f. We found a significant correlation between α_f and α_Q in the damaged specimens when they were measured in dry or in wet conditions. Such a correlation between α_f and α_Q has already been described in various damaged material (Van den Abeele et al., 2009, 2001a; Van den Abeele and De Visscher, 2000). Like Van den Abeele et al. (2009), we report a lower sensitivity of α_Q to crack length, in comparison to α_f.

Nonlinear resonant ultrasound spectroscopy is suitable for a multimodal approach (Rivière et al., 2010) as each resonant mode generates a different strain field. In this report, we focus the analysis on the first compression mode. But other resonant modes can be measured. For example, we measured also the second and third compression modes. The results obtained with these modes were similar to the results obtained by processing the first compression mode (data not shown). These results are consistent with the theory (Liu et al., 2010; Van den Abeele, 2007). Indeed, the value of the measured nonlinear parameter depends on the local strain field: if the crack is located in a node of the strain field, the crack would not be excited by opening/closing and no nonlinear hysteretic behavior would be measured. In fixed–free boundary conditions, the strain field is identical for the three modes in the center of the specimens where the crack is localized. It means that the value of the nonlinear parameter must be the same for the three modes. Different nonlinear elastic behavior would be expected under symmetric boundary conditions (free–free or fixed–fixed) as the local strain fields may vary depending on the mode (Liu et al., 2010; Van den Abeele, 2007; Van den Abeele et al., 2004).

Although NRUS most often exploits the first compression mode (or Pochammer–Chree mode for cylinder), other modes have also been exploited, such as flexural mode (Van den Abeele et al., 2009, 2001b). In this study, the nonlinear hysteretic behavior of our specimens has also been investigated using the flexural mode (data not shown). The nonlinear hysteretic parameters extracted from this mode were similar to those derived from the compression mode. Indeed, in case of flexural modes, shear stresses exist but remain weak such that they are generally neglected. This may explain why the nonlinear elastic parameters measured in compression and flexural modes are similar, as we observed it in this study. They reflect mostly the nonlinear longitudinal elastic behavior of the specimens. For both compression and flexural modes, the activation of the nonlinear hysteretic behavior is mainly controlled by opening/closing mechanism due to the longitudinal traveling wave, while the friction mechanisms due to shear stresses remained too small. In order to investigate selectively the sensitivity of shear elastic coefficients to the nonlinear hysteretic behavior, one would have to perform NRUS measurements with torsion resonant modes for instance.

5. Conclusion

The results described in this study provide new insights into the nonlinear elastic behavior of human cortical bone. The proposed experimental protocol allowed the concurrent assessment of acoustic nonlinear parameters reflecting hysteretic elasticity of human cortical bone specimens subject to a crack initiation and propagation. SR-μCT was used to assess crack lengths and orientations at the end of the toughness test. Results showed a significant correlation between the nonlinear hysteretic elasticity of bone and crack length. NRUS is a promising minimally invasive approach for assessing microdamage in situ. Although the results relate primarily to the characterization of bone, they can be useful for other materials such as metals, composites or concrete.

Acknowledgments

The authors are grateful to G. Renaud and J. Rivière for their helpful comments and suggestions during the preparation of the experiments, as well as P.A. Johnson, Los Alamos National Laboratory, NM, USA for fruitful discussions and E. Boller, M. Zuluaga and M. Langer for help during the ESRF experiment performed in the framework of LTP MD431. This research was supported by the Agence Nationale de la Recherche (ANR), France (Grant BONUS_07BLAN0197).

REFERENCES

Achenbach, J., 1984. Wave Propagation in Elastic Solids. Elsevier, North-Holland.

Antonaci, P., Bruno, C., Bocca, P., Scalerandi, M., Gliozzi, A., 2010. Nonlinear ultrasonic evaluation of load effects on discontinuities in concrete. Cem. Concr. Res. 40, 340–346.

Aymerich, F., Staszewski, W., 2010. Experimental study of impact-damage detection in composite laminates using a cross-modulation vibro-acoustic technique. Struct. Health Monit. 9, 541.

Bentahar, M., El Guerjouma, R., 2009. Monitoring progressive damage in polymer-based composite using nonlinear dynamics and acoustic emission. J. Acoust. Soc. Am. 125, EL39.

Burr, D., 2011. Why bones bend but don't break. J. Musculoskelet. Neuronal Interact. 11, 270–285.

Burr, D.B., Turner, C.H., Naick, P., Forwood, M.R., Ambrosius, W., Hasan, M.S., Pidaparti, R., 1998. Does microdamage accumulation affect the mechanical properties of bone?. J. Biomech. 31, 337–345.

Cantrell, J.H., 2006. Dependence of microelastic–plastic nonlinearity of martensitic stainless steel on fatigue damage accumulation. J. Appl. Phys. 100, 063508.

Cantrell, J., Yost, W., 2001. Nonlinear ultrasonic characterization of fatigue microstructures. Int. J. Fatigue 23, 487–490.

Cardoso, L., Herman, B.C., Verborgt, O., Laudier, D., Majeska, R.J., Schaffler, M.B., 2009. Osteocyte apoptosis controls activation of intracortical resorption in response to bone fatigue. J. Bone Miner. Res. 24, 597–605.

Chapurlat, R., Delmas, P., 2009. Bone microdamage: a clinical perspective. Osteoporos. Int. 20, 1299–1308.

Chen, J., Jayapalan, A.R., Kim, J.Y., Kurtis, K.E., Jacobs, L.J., 2010. Rapid evaluation of alkali-silica reactivity of aggregates using a nonlinear resonance spectroscopy technique. Cem. Concr. Res. 40, 914–923.

Courtney, C., Drinkwater, B., Neild, S., Wilcox, P., 2008. Factors affecting the ultrasonic intermodulation crack detection technique using bispectral analysis. NDT E Int. 41, 223–234.
Currey, J.D., 1988. The effect of porosity and mineral content on the Young's modulus of elasticity of compact bone. J. Biomech. 21, 131–139.
Derome, D., Griffa, M., Koebel, M., Carmeliet, J., 2011. Hysteretic swelling of wood at cellular scale probed by phase-contrast X-ray tomography. J. Struct. Biol. 173, 180–190.
Diab, T., Vashishth, D., 2005. Effects of damage morphology on cortical bone fragility. Bone 37, 96–102.
Donskoy, D., Sutin, A., Ekimov, A., 2001. Nonlinear acoustic interaction on contact interfaces and its use for nondestructive testing. NDT E Int. 34, 231–238.
Duffour, P., Morbidini, M., Cawley, P., 2006. A study of the vibro-acoustic modulation technique for the detection of cracks in metals. J. Acoust. Soc. Am. 119, 1463.
Fletcher, L., Codrington, J., Parkinson, I., 2014. Effects of fatigue induced damage on the longitudinal fracture resistance of cortical bone. J. Mater. Sci. Mater. Med. 25, 1661–1670, http://dx.doi.org/10.1007/s10856-014-5213-5.
Frouin, J., Sathish, S., Matikas, T.E., Na, J.K., 1999. Ultrasonic linear and nonlinear behavior of fatigued Ti–6Al–4V. J. Mater. Res. 14, 1295–1298.
Griffin, L.V., Gibeling, J.C., Gibson, V.A., Martin, R.B., Stover, S.M., 1997. Artifactual nonlinearity due to wear grooves and friction in four-point bending experiments of cortical bone. J. Biomech. 30, 185–188.
Grimal, Q., Haupert, S., Mitton, D., Vastel, L., Laugier, P., 2009. Assessment of cortical bone elasticity and strength: mechanical testing and ultrasound provide complementary data. Med. Eng. Phys. 31, 1140–1147.
Gupta, H., Zioupos, P., 2008. Fracture of bone tissue: the 'hows' and the 'whys'. Med. Eng. Phys. 30, 1209–1226.
Guyer, R.A., Johnson, P.A., 2009. Nonlinear Mesoscopic Elasticity: The Complex Behaviour of Rocks, Soil, Concrete. Wiley-VCH, Weinheim.
Haupert, S., Guérard, S., Peyrin, F., Mitton, D., Laugier, P., 2014. Non destructive characterization of cortical bone micro-damage by nonlinear resonant ultrasound spectroscopy. PLoS ONE 9, e83599, http://dx.doi.org/10.1371/journal.pone.0083599.
Haupert, S., Renaud, G., Riviere, J., Talmant, M., Johnson, P.A., Laugier, P., 2011. High-accuracy acoustic detection of nonclassical component of material nonlinearity. J. Acoust. Soc. Am. 130, 2654–2661.
Hernandez, C.J., Lambers, F.M., Widjaja, J., Chapa, C., Rimnac, C.M., 2014. Quantitative relationships between microdamage and cancellous bone strength and stiffness. Bone 66, 205–213, http://dx.doi.org/10.1016/j.bone.2014.05.023.
Johnson, P.A., Zinszner, B., Rasolofosaon, P., Cohen-Tenoudji, F., Van Den Abeele, K., 2004. Dynamic measurements of the nonlinear elastic parameter alpha in rock under varying conditions. J. Geophys. Res.-Solid Earth 109, B02202.
Johnson, P., Sutin, A., 2005. Slow dynamics and anomalous nonlinear fast dynamics in diverse solids. J. Acoust. Soc. Am. 117, 124–130.
Kim, J.Y., Jacobs, L.J., Qu, J., Littles, J.W., 2006. Experimental characterization of fatigue damage in a nickel-base superalloy using nonlinear ultrasonic waves. J. Acoust. Soc. Am. 120, 1266.
Kim, J.Y., Yakovlev, V., Rokhlin, S., 2004. Surface acoustic wave modulation on a partially closed fatigue crack. J. Acoust. Soc. Am. 115, 1961.
Larrue, A., Rattner, A., Peter, Z.A., Olivier, C., Laroche, N., Vico, L., Peyrin, F., 2011. Synchrotron radiation micro-CT at the micrometer scale for the analysis of the three-dimensional morphology of microcracks in human trabecular bone. PLoS ONE 6, 21297.
Lee, T.C., Mohsin, S., Taylor, D., Parkesh, R., Gunnlaugsson, T., O'Brien, F.J., Giehl, M., Gowin, W., 2003. Detecting microdamage in bone. J. Anat. 203, 161–172.
Lee, T.C., O'Brien, F.J., Taylor, D., 2000. The nature of fatigue damage in bone. Int. J. Fatigue 22, 847–853.
Liu, X., Dao, Z., Zhu, J., Qu, W., Gong, X., Van Den Abeele, K., Ma, L., 2010. Localization of material defects using nonlinear resonant ultrasound spectroscopy under asymmetric boundary conditions. Phys. Procedia 3, 55–61.
Meijering, E., 2010. Neuron tracing in perspective. Cytometry A 77, 693–704.
Meng, X., Rosenthal, R., Rubin, D.B., 1992. Comparing correlated correlation coefficients. Psychol. Bull. 111, 172–175, http://dx.doi.org/10.1037/0033-2909.111.1.172.
Meo, M., Polimeno, U., Zumpano, G., 2008. Detecting damage in composite material using nonlinear elastic wave spectroscopy methods. Appl. Compos. Mater. 15, 115–126.
Moreschi, H., Callé, S., Guerard, S., Mitton, D., Renaud, G., Defontaine, M., 2011. Monitoring trabecular bone microdamage using a dynamic acousto-elastic testing method. Proc. Inst. Mech. Eng. H 225, 1–12.
Muller, M., Mitton, D., Talmant, M., Johnson, P., Laugier, P., 2008. Nonlinear ultrasound can detect accumulated damage in human bone. J. Biomech. 41, 1062–1068.
Nagy, P.B., 1998. Fatigue damage assessment by nonlinear ultrasonic materials characterization. Ultrasonics 36, 375–381.
Nazarov, V., 2001. Acoustic nonlinearity of cracks partially filled with liquid: cubic approximation. J. Acoust. Soc. Am. 109, 2642.
Nazarov, V., Radostin, A., 2008. Acoustic nonlinearity of water-like materials with partially liquid-filled capillaries. Acoust. Phys 54, 460–463.
O'Brien, F.J., Taylor, D., Lee, T.C., 2007. Bone as a composite material: the role of osteons as barriers to crack growth in compact bone. Int. J. Fatigue 29, 1051–1056.
O'Brien, F.J., Taylor, D., Lee, T.C., 2002. An improved labelling technique for monitoring microcrack growth in compact bone. J. Biomech. 35, 523–526.
Payan, C., Garnier, V., Moysan, J., 2010. Effect of water saturation and porosity on the nonlinear elastic response of concrete. Cem. Concr. Res. 40, 473–476.
Renaud, G., Calle, S., Remenieras, J.P., Defontaine, M., 2008. Non-linear acoustic measurements to assess crack density in trabecular bone. Int. J. Non-Linear Mech. 43, 194–200.
Rho, J.Y., Pharr, G.M., 1999. Effects of drying on the mechanical properties of bovine femur measured by nanoindentation. J. Mater. Sci. Mater. Med. 10, 485–488.
Rivière, J., Renaud, G., Haupert, S., Talmant, M., Laugier, P., Johnson, P., 2010. Nonlinear acoustic resonances to probe a threaded interface. J. Appl. Phys. 107, 4901.
Sagar, S.P., Metya, A., Ghosh, M., Sivaprasad, S., 2011. Effect of microstructure on non-linear behavior of ultrasound during low cycle fatigue of pearlitic steels. Mater. Sci. Eng. A 528, 2895–2898.
Shane, E., Burr, D., Ebeling, P.R., Abrahamsen, B., Adler, R.A., Brown, T.D., Cheung, A.M., Cosman, F., Curtis, J.R., Dell, R., 2010. Atypical subtrochanteric and diaphyseal femoral fractures: report of a task force of the American society for bone and mineral research. J. Bone Miner. Res. 25, 2267–2294.
Straka, L., Yagodzinskyy, Y., Landa, M., Hänninen, H., 2008. Detection of structural damage of aluminum alloy 6082 using elastic wave modulation spectroscopy. NDT E Int. 41, 554–563.
Tutuncu, A.N., Podio, A.L., Sharma, M.M., 1998. Nonlinear viscoelastic behavior of sedimentary rocks, Part II: hysteresis effects and influence of type of fluid on elastic moduli. Geophysics 63, 195–203.
Ulrich, T.J., Johnson, P.A., Muller, M., Mitton, D., Talmant, M., Laugier, P., 2007. Application of nonlinear dynamics to monitoring progressive fatigue damage in human cortical bone. Appl. Phys. Lett. 91, 213901–213904.
Van den Abeele, K., 2007. Multi-mode nonlinear resonance ultrasound spectroscopy for defect imaging: an analytical

approach for the one-dimensional case. J. Acoust. Soc. Am. 122, 73–90.
Van den Abeele, K., Carmeliet, J., Johnson, P., Zinszner, B., 2002. Influence of water saturation on the nonlinear elastic mesoscopic response in Earth materials and the implications to the mechanism of nonlinearity. J. Geophys. Res. 107, 2121.
Van den Abeele, K., Carmeliet, J., Ten Cate, J.A., Johnson, P.A., 2000. Nonlinear elastic wave spectroscopy (NEWS) techniques to discern material damage, Part II: single-mode nonlinear resonance acoustic spectroscopy. Res. Nondestruct. Eval. 12, 31–42.
Van den Abeele, K., De Visscher, J., 2000. Damage assessment in reinforced concrete using spectral and temporal nonlinear vibration techniques. Cem. Concr. Res. 30, 1453–1464.
Van den Abeele, K., Le Bas, P., Van Damme, B., Katkowski, T., 2009. Quantification of material nonlinearity in relation to microdamage density using nonlinear reverberation spectroscopy: experimental and theoretical study. J. Acoust. Soc. Am. 126, 963.
Van den Abeele, K., Schubert, F., Aleshin, V., Windels, F., Carmeliet, J., 2004. Resonant bar simulations in media with localized damage. Ultrasonics 42, 1017–1024.
Van den Abeele, K., Sutin, A., Carmeliet, J., Johnson, P.A., 2001a. Micro-damage diagnostics using nonlinear elastic wave spectroscopy (NEWS). NDT E Int. 34, 239–248.
Van den Abeele, K., Van de Velde, K., Carmeliet, J., 2001b. Inferring the degradation of pultruded composites from dynamic nonlinear resonance measurements. Polym. Compos. 22, 555–567.
Vashishth, D., 2004. Rising crack-growth-resistance behavior in cortical bone: implications for toughness measurements. J. Biomech. 37, 943–946.
Verborgt, O., Gibson, G.J., Schaffler, M.B., 2000. Loss of osteocyte integrity in association with microdamage and bone remodeling after fatigue in vivo. J. Bone Miner. Res. 15, 60–67.
Voide, R., Schneider, P., Stauber, M., Wyss, P., Stampanoni, M., Sennhauser, U., van Lenthe, G.H., Müller, R., 2009. Time-lapsed assessment of microcrack initiation and propagation in murine cortical bone at submicrometer resolution. Bone 45, 164–173, http://dx.doi.org/10.1016/j.bone.2009.04.248.
Yeni, Y.N., Fyhrie, D.P., 2002. Fatigue damage-fracture mechanics interaction in cortical bone. Bone 30, 509–514.
Zagrai, A., Donskoy, D., Chudnovsky, A., Golovin, E., 2008. Micro-and macroscale damage detection using the nonlinear acoustic vibro-modulation technique. Res. Nondestruct. Eval. 19, 104–128.
Zardan, J.P., Payan, C., Garnier, V., Salin, J., 2010. Effect of the presence and size of a localized nonlinear source in concrete. J. Acoust. Soc. Am. 128, EL38–EL42, http://dx.doi.org/10.1121/1.3448024.
Zinszner, B., Johnson, P.A., Rasolofosaon, P.N.J., 1997. Influence of change in physical state on elastic nonlinear response in rock: significance of effective pressure and water saturation. J. Geophys. Res.-Solid Earth 102, 8105–8120.
Zioupos, P., 2001. Accumulation of in-vivo fatigue microdamage and its relation to biomechanical properties in ageing human cortical bone. J. Microsc. 201, 270–278.